The mixed finite element method applied to the Stokes flow

Project report

Mohamed Yassine Letaief and Sofiane Dhouib
Denis Matignon and Ghislain Haine

Abstract

This paper deals with the use of the finite element method to simulate the Stokes flow. It begins with a mathematical study of the existence and uniqueness of a solution of the Stokes equations, i.e the pressure and velocity fields of such flow. Strong and weak formulations of the problem are given. The proper conditions used in the mixed finite element method applied to these equations are detailed in the first section of this paper. Different configurations of the Stokes flow are simulated in order to demonstrate the importance of effectuating the proper choices for pressure and velocity finite dimensional subspaces before running a simulation. The work has been extended to simulate steady Navier-Stokes flow. The non linear term in Navier-Stokes equations is taken into account using two different algorithms: Newton and Picard methods.

Keywords: Mixed finite element method, Stokes flow, inf-sup condition, LBB condition, Navier-Stokes, Newton-Raphson method, Picard method

Introduction

The Stokes flow is a steady incompressible flow, characterized by a Reynolds number very inferior to one. In other words, the advective inertial forces are negligible compared with the viscous forces. This kind of flow is obtained when the viscosity is very high, the velocity is very low or when the length scales of the flow are very small. The Stokes flow has concrete applications in a variety of fields such as geophysics (study of lava flow), biology (movement of micro-organisms) or the study of lubricants.

Computational fluid dynamics is increasingly used in the study of flows. Numerical simulation has a lower cost than physical experiments. For instance, changing the experimental conditions in the simulations usually requires changing few lines in the program, whereas in the physical word, a whole new experience has to be performed. The information it provides is particularly valuable when there is no explicit analytical solution, which is the case for a wide range of equations.

Moreover the numerical simulations provide rapid, reliable and easy to use results.

The velocity and the pressure fields of the flow mentioned above can be calculated using the finite elements method.

1 Theoretical study of the Stokes flow

1.1 From Navier-Stokes to Stokes

Newtonian fluids motion is governed by the Navier-Stokes equations. These equations are particularly complex to resolve, even in some simple cases, because of the presence of non-linear terms. We give below the momentum and the mass conservation equations for an incompressible flow, where $\mathbf{u} = (u_1, ..., u_N)(N = 2, 3)$,$p$,$\mu$ and $\mathbf{f}$ are respectively the velocity field, the pressure field, the dynamic viscosity of the fluid and the body force. Ω is the domain occupied by the fluid, supposed to be an open bounded set of $\mathbb{R}^N$, with a sufficiently smooth boundary $\partial\Omega$

$$\begin{aligned} \rho\left(\frac{\partial \mathbf{u}}{\partial t} + (\mathbf{u}.\nabla)\mathbf{u}\right) - \mu\Delta\mathbf{u} + \nabla p = \mathbf{f} \qquad & \text{in } \Omega \\ \nabla.\mathbf{u} = 0 \qquad & \text{in } \Omega \\ \mathbf{u} = 0 \qquad & \text{on } \partial\Omega \end{aligned}$$

The last boundary condition means that we consider the flow in the reference frame of Ω.

To compare the contributions of the different terms appearing in these equations, we procede with a nondimensionalization.
Let U, L and T be the velocity, the length and the time that characterize the flow. We use the following nondimensionalizations : $\tilde{\mathbf{u}} = \frac{\mathbf{u}}{U}$, $\tilde{t} = \frac{t}{T}$, $\tilde{x} = \frac{x}{L}$ (the same goes for y and z). The nondimensionalization we use for the pressure consists in saying that the pressure and

the viscosity stresses have the same order of magnitude. The total stress exerced on fluid is given by $\mu\Delta\mathbf{u} + \nabla p$. In terms of order of magnitude, this can be written as $\mu\frac{U}{L^2} + p/L$. Hence, we have $\tilde{p} = \frac{p}{\frac{\mu U}{L}}$, as seen in [4]. The nondimensionalization leads to the following equations

$$Re\left(\frac{\partial\tilde{\mathbf{u}}}{\partial\tilde{t}} + (\tilde{\mathbf{u}}.\tilde{\nabla})\tilde{\mathbf{u}}\right) - \tilde{\Delta}\tilde{\mathbf{u}} + \tilde{\nabla}\tilde{p} = \tilde{\mathbf{f}} \qquad \text{in } \Omega \qquad (1)$$

$$\tilde{\nabla}.\tilde{\mathbf{u}} = 0 \qquad \text{in } \Omega \qquad (2)$$

Here, $\tilde{\mathbf{f}} = \frac{\mathbf{f}}{\frac{\mu U}{L^2}}$ and $Re = \frac{\rho UL}{\mu} = \frac{UL}{\nu}$ denotes the Reynolds number of the flow (ν is the kinematic viscosity). This number plays a major role in this study, as it allows to define the Stokes flow properly:
We can consider a Stokes flow when $Re \ll 1$. In other words, the advective inertial forces are negligible compared with the viscosity stresses. The equations 1 and 2 become

$$-\Delta\mathbf{u} + \nabla p = \mathbf{f} \qquad \text{in } \Omega \qquad (3)$$

$$\nabla.\mathbf{u} = 0 \qquad \text{in } \Omega \qquad (4)$$

$$\mathbf{u} = 0 \qquad \text{on } \partial\Omega \qquad (5)$$

Here, we omit the $\tilde{}$ symbol to simplify the equations, but we always consider nondimensionalized quantities.

This system of equations consists the strong formulation of the Stokes equations of an incompressible flow. In the next section, we give the weak formulation of these equations, to prepare for the numerical resolution.

1.2 Continuous weak formulation and LBB condition

Let $\mathbf{u}$ and p be the unknown velocity and pressure fields of the Stokes flow. The boundary condition verified by $\mathbf{u}$ lead to the choice $\mathbf{u} \in H_0^1(\Omega)^N$. Also, we notice that if p is a solution, then $p + c$ is also a solution, where c is a constant. In order to guarantee its uniqueness, we searcha pressure field with a null mean, i.e $p \in \dot{L^2}(\Omega) = \left\{p \in L^2(\Omega); \int_\Omega p = 0\right\}$. Physically speaking, the pressure is a positive quantity, and it can be written as $p = \bar{p} + \hat{p}$, where $\bar{p}$ is the mean value of the pressure in Ω, and thus it is a constant. That's why in our equations we only deal with the term $\hat{p}$ (simply noted p).

Thus, the weak formulation consists in finding $(\mathbf{u}, p) \in H_0^1(\Omega)^N \times \dot{L^2}(\Omega)$ such that :

$$\int_\Omega \nabla\mathbf{u} : \nabla\mathbf{v} - \int_\Omega p\nabla.\mathbf{v} = \int_\Omega \mathbf{f}.\mathbf{v} \qquad \forall\mathbf{v} \in H_0^1(\Omega)^N \qquad (6)$$

$$\int_\Omega q\nabla.\mathbf{u} = 0 \qquad \forall q \in \dot{L^2}(\Omega) \qquad (7)$$

If we denote $H_0^1(\Omega)^N$ and $\dot{L^2}(\Omega)$ respectively by V and S. This system can be written as :

$$a(\mathbf{u}, \mathbf{v}) + b(\mathbf{v}, p) = l_{\mathbf{f}}(v) \qquad \forall\mathbf{v} \in V \qquad (8)$$

$$b(\mathbf{u}, q) = 0 \qquad \forall q \in S \qquad (9)$$

where :

$$a : V \times V \to \mathbb{R}$$
$$(\mathbf{u}, \mathbf{v}) \mapsto \int_\Omega \nabla\mathbf{u} : \nabla\mathbf{v}$$

$$b : V \times S \to \mathbb{R}$$
$$(\mathbf{v}, p) \mapsto -\int_\Omega p\nabla.\mathbf{v}$$

$$l_{\mathbf{f}} : V \to \mathbb{R}$$
$$\mathbf{v} \mapsto \int_\Omega \mathbf{f}.\mathbf{v}$$

. It can be shown that $a(.,.)$ is a coercive continuous bilinear form and that $l_{\mathbf{f}}$ is a continuoues linear form, which suggests to apply the Lax-Milgram theorem. However, $b(.,.)$ must also be continuous and verifying a certain condition known as the Ladizhenskaya-Babushka-Brezzi condition, or the inf-sup condition, in order to guarantee the existence and uniqueness of the solution.

A bilinear form $\varphi : X \times Y \to \mathbb{R}$ (where X and Y) are two Hilbert spaces) verifies the inf-sup condition if there is a constant $\beta > 0$ such that :

$$\inf_{q\in Y\setminus\{0\}}\left(\sup_{\mathbf{v}\in X\setminus\{0\}}\frac{|\varphi(\mathbf{v}, q)|}{\| \mathbf{v} \|_X \| q \|_Y}\right) \geq \beta \qquad (10)$$

which is equivalent to the condition :

$$\forall q \in Y, \sup_{\mathbf{v}\in X\setminus\{0\}}\frac{|\varphi(\mathbf{v}, q)|}{\| \mathbf{v} \|_X} \geq \beta \| q \|_Y \qquad (11)$$

The pressure field can be seen as a Lagrange multiplier of the divergence free condition when we consider the following optimization problem:

$$\underset{\mathbf{u}\in V}{\text{minimize}}\ \frac{1}{2}a(\mathbf{u}, \mathbf{u}) - l_{\mathbf{f}}(\mathbf{u}) \qquad (12)$$

$$\text{subject to } \nabla.\mathbf{u} = 0 \qquad (13)$$

Remark : The homogeneous boundary condition can be generalized to a non-homogeneous one, meaning $\mathbf{u} = \mathbf{g}$ on Ω, where g is a given function. In this case, we use the decomposition $\mathbf{u} = \mathbf{u}_0 + \mathbf{u}_d$, where $\mathbf{u}_d$ is a known function verifying the non-homogeneous Dirichlet condition.

1.3 Discrete weak formulation

In order to run a finite elements simulation it is necessary to choose finite dimensional subspaces of V and S for the velocity and the pressure. let these subspaces be V_h (velocity) and S_h (pressure). The discrete weak formulation is:

Find $(\mathbf{u}, p) \in V_h \times S_h$ such that

$$a(\mathbf{u}_h, \mathbf{v}_h) + b(\mathbf{v}_h, p_h) = l_{\mathbf{f}}(\mathbf{v}_h) \qquad \forall\mathbf{v}_h \in V_h \qquad (14)$$

$$b(\mathbf{u}_h, q_h) = 0 \qquad \forall q_h \in S_h \qquad (15)$$

Since V_h and S_h are closed subspaces of V and S, they're Hilbert spaces. Thus, $a(.,.)$ and $b(.,.)$ must again verify the conditions we mentioned in section 1.2 in the finite dimensional subspaces.
In particular, $b(.,.)$ must verify the inf-sup condition on $V_h \times S_h$: $\exists \beta > 0$;

$$\forall q_h \in S_h \subset S, \quad \sup_{\mathbf{v}_h \in V_h \setminus \{0\}} \frac{|b(\mathbf{v}_h, q_h)|}{\| \mathbf{v}_h \|_{V_h}} \geq \beta \| q_h \|_{S_h} \tag{16}$$

Whereas we have

$$\forall q_h \in S_h \subset S, \quad \sup_{\mathbf{v} \in V \setminus \{0\}} \frac{|b(\mathbf{v}, q_h)|}{\| \mathbf{v} \|_{V}} \geq \beta \| q_h \|_{S_h} \tag{17}$$

The problem here is that $\forall q_h \in S_h, \quad \sup_{\mathbf{v}_h \in V_h \setminus \{0\}} \frac{|b(\mathbf{v}_h, q_h)|}{\|\mathbf{v}_h\|_{V_h}} \leq \sup_{\mathbf{v}_h \in V \setminus \{0\}} \frac{|b(\mathbf{v}_h, q_h)|}{\|\mathbf{v}\|_{V_h}}$, because $V_h \subset V$. Thus if we have 17, we don't necessarily have 16. Consequently, the subspaces V_h and S_h must verify a certain compatibility.

Let N_h and K_h be the dimensions of respectively V_h and S_h , $\{\varphi_1, ..., \varphi_{N_h}\}$ and $\{\psi_1, ..., \psi_{K_h}\}$ their associated basis.
Then we have $p_h = \sum_{i=1}^{K_h} p_i \psi_i$ and $\mathbf{u}_h = \sum_{i=1}^{N_h} u_i \varphi_i$. The resolution of the problem consists in solving the following matrix system:

$$AU + B^T P = F \tag{18}$$
$$BU = 0 \tag{19}$$

Where $A \in \mathbb{R}^{N_h \times N_h}$ is defined by $(A)_{ij} = a(\varphi_i, \varphi_j)$. Since $a(.,.)$ is a symmetric coercive bilinear form, A is a symmetric positive-definite matrix. $B \in \mathbb{R}^{N_h \times K_h}$ is a rectangular matrix defined by $(B)_{ij} = b(\varphi_j, \psi_i)$. $F \in \mathbb{R}^{\mathbb{N}\sim}$ is defined by $F_i = l_{\mathbf{f}}(\varphi_i)$, $U = (u_1, ..., u_{N_h})$ and $P = (p_1, ..., p_{K_h})$.
This can also be put under the form :

$$\begin{pmatrix} A & B^T \\ B & 0 \end{pmatrix} \begin{pmatrix} U \\ P \end{pmatrix} = \begin{pmatrix} F \\ 0 \end{pmatrix} \tag{20}$$

Where $C = \begin{pmatrix} A & B^T \\ B & 0 \end{pmatrix}$ is a square matrix of size $N_h + K_h$.
In order to guarantee the existence and uniqueness of a solution for this problem, the matrix C must be invertible. This condition is true if and only if B^T has full column rank. We give below the proof of this assertion.

Proof. A is an invertible matrix so the previous problem can be rewritten as follows:

$$U = A^{-1}(F - B^T P) \tag{21}$$
$$BA^{-1}B^T P = BA^{-1}F \tag{22}$$

We notice that the linear problem has a unique solution, meaning that C is invertible, if and only if $R = BA^{-1}B^T$ is invertible. So if we show that R is invertible if and only if $\ker(B^T) = 0$, the proof is finished.

If $\ker(B^T) = 0$ then $P^T BA^{-1}B^T P > 0 \ \forall P \in \mathbb{R}^{K_h}$,because A is a symmetric positive-definite matrix. which means that R is positive-definite, so it is invertible. Thus C is invertible.
However, if $\ker(B^T) \neq 0$, then $\exists p_0 \in \mathbb{R}^{K_h} \setminus \{0\}; B^T p_0 = 0$, so $Rp_0 = 0$, thus R is not invertible. □

It is shown below (a part of the proof is given in [13]) that the condition B^T has full column rank is equivalent to the discrete inf-sup condition.

Proof. We will show that $\ker(B^T) \neq \{0\}$ if and only if the discrete inf-sup condition is not repected.

$$\begin{aligned} \ker(B^T) \neq 0 &\Leftrightarrow \exists P \neq 0 \in \mathbb{R}^{K_h}; B^T P = 0 \\ &\Leftrightarrow \exists P \neq 0 \in \mathbb{R}^{K_h}; \sum_{j=1}^{K_h} b(\varphi_i, \psi_j) = 0, \ \forall i \leq N_h \\ &\Leftrightarrow \exists p_h \in S_h \setminus \{0\}; b(\varphi_i, p_h) = 0 \ \forall i \leq N_h \\ &\Leftrightarrow \exists p_h \in S_h \setminus \{0\}; b(\mathbf{v}_h, p_h) = 0 \ \forall \mathbf{v}_h \in V_h, \mathbf{v}_h \neq 0. \end{aligned}$$

It is clear that the inf-sup condition isn't verified in this case. □

The fact that B^T has full column rank implies that $N_h \geq K_h$.

1.3.1 Choice of finite dimensional subspaces for the velocity and the pressure

There are several choices for the subspaces V_h and S_h, for example :

- $\mathbb{P}_2/\mathbb{P}_0$: A simple element.
- $\mathbb{P}_{k+1}/\mathbb{P}_k$ for $k \geq 1$: Taylor-Hood element.
- $\mathbb{P}_1 - bubble/\mathbb{P}_1$, where $\mathbb{P}_1 - bubble = \mathbb{P}_1 \oplus \mathbb{R}.\lambda_1\lambda_2\lambda_3$: We add a degree of freedom to the velocity field on each triangle of the mesh. We denote $\lambda_1\lambda_2\lambda_3$ by $\mathscr{B}$.

We give a proof (found in [3]) that B^T has full column rank with the choice $\mathbb{P}_1 - bubble/\mathbb{P}_1$.

Proof. Let $q \in S_h$ such that

$$b(\mathbf{v}, q) = -\int_\Omega q \nabla.\mathbf{v} = 0 \ \forall \mathbf{v} \in V_h.$$

If we take $\mathbf{v} = \mathscr{B}$ (bubble function), then we have :

$$\int_K q \left(A\frac{\partial \beta}{\partial x} + B\frac{\partial \beta}{\partial y} \right) \ \forall (A, B) \in \mathbb{R}^2$$

for every traingle K of the mesh.
After an integration by parts, and since $\mathscr{B}$ is null on the border of K, we obtain :

$$-\int_K \frac{\partial q}{\partial x} A.\mathscr{B} - \int_K \frac{\partial q}{\partial y} B.\mathscr{B}, \ \forall (A, B) \in \mathbb{R}^2$$

Hence $\int_K \frac{\partial q}{\partial x}\mathscr{B} = 0$ and $\int_K \frac{\partial q}{\partial y}\mathscr{B} = 0$. We know that the partial derivatives of q are constants on every triangle, since $q \in \mathbb{P}_1$, and that $\int_K \mathscr{B} = \frac{9}{20}|K|$. This implies that $\frac{\partial q}{\partial x} = \frac{\partial q}{\partial y} = 0$ on every triangle K. q is then a piecewise constant, but it is continuous on Ω, thus $q = 0$. This shows that $\ker(B^T) = \{0\}$. □

$\mathbb{P}_1/\mathbb{P}_1$ and $\mathbb{P}_1/\mathbb{P}_0$ are incomptaible subspaces that may cause a velocity locking, meaning that the velocity field becomes null on Ω. A proof of this phenomenon can be found in

1.3.2 Taking the null pressure mean into account

Let $M \in \mathbb{R}^{K_h \times K_h}; (M)_{i,j} = \int_\Omega \psi_i \psi_j$. Then

$$\forall p_h \in S_h, \int_\Omega p_h = (1, ..., 1)MP \tag{23}$$

(we keep the same notations used in 18).
A null pressure means $(1, ..., 1)MP = (1, ..., 1)(BA^{-1}B^T)^{-1}BA^{-1}F = 0$. However, this condition is verified for a limited possibilities for F. In general, it is not verified. Thus, we impose this condition by solving a slightly different equation, after changing equation 5 , as seen in [13].

$$\nabla.\mathbf{u} = \varepsilon p \text{ in } \Omega \tag{24}$$

Where $0 < \varepsilon \ll 1$. We lose the exact divergence free condition for the veloity but we guarantee that the pressure is a null mean function:

$$\int_\Omega \nabla.\mathbf{u} = \underbrace{\int_{\partial\Omega} \mathbf{u}.\mathbf{n} = 0}_{\text{boundary condition}} = \varepsilon \int_\Omega p \tag{25}$$

The matrix C then becomes $C = \begin{pmatrix} A & B^T \\ B & -\varepsilon I_{K_h} \end{pmatrix}$. After the simulation is performed we should verify that the divergence of the velocity can be be negligible. This means that the pressure is not too high, which allows us to write $\varepsilon.p \ll 1$.

After choosing compatible spaces for the velocity and the pressure, it is possible to proceed to the numerical simulation itself.
All the simulation are performed with FreeFem++

2 Numerical implementations

2.1 The software FreeFem++

The software FreeFem++ is a free software developed by F.Hecht. It is a numerical solver used to solve partial differential equations in dimensions 2 and 3, and a high level programming language well adapted to variational formulations.
FreeFem++ is very intuitive and close to the mathematical formulation which makes it easier to use. Also it has an automatic mesh generator that only demands the border and number of nods on it as an input parameter.
Below is a mesh generated with FreeFem for a NACA0012 airfoil inside a wind tunnel. We can see that the density of the mesh is higher close to the air foil in order to capture the potential fast variations of velocity and pressure in this zone.

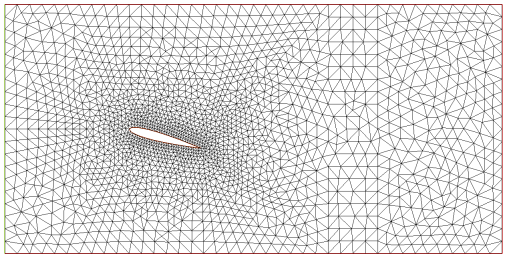

Figure 1: Mesh generated with FreeFem for a NACA0012 airfoil inside a wind tunnel
.

2.2 Simulations of the steady Stokes flow

In this section, we deal with various physical examples of the stready 2D stokes flow. For each example, we simulated the fluid motion with different finite dimensional subspaces, including :
$\mathbb{P}_1 - bubble/\mathbb{P}_1$, $\mathbb{P}_2/\mathbb{P}_1$, $\mathbb{P}_1/\mathbb{P}_0$, $\mathbb{P}_1/\mathbb{P}_1$
For the first and second examples, we give the L^2 errors between the numerically calculated fields and the analytically calculated ones ($\| (p_{numerical} - p_{analytical}) \|_{L^2(\Omega)}$ for the pressure for example). Also, without a loss of generality, we suppose that $\rho = 1$.
We use the penalised set of equations in order to obtain a pressure field with a null mean.We noticed that the relaxation of the divergence free condition) stabilises the solution even with a very small ε values (for example $\varepsilon = 10^{-10}$)

2.2.1 Rotating cylinder

We consider a fluid contained in a cylinder with a radius R, long enough to consider a 2D flow. Hence, $\Omega \in \mathbb{R}^2$ is a circle with a radius R. The cylinder is rotating around its own axis at an angular velocity ω , subjecting the fluid to a centrifugal body force $\mathbf{f}$ in the cylinder-fixed frame of reference $(\mathbf{u}_r, \mathbf{u}_\theta, \mathbf{u}_z)$. We have $\mathbf{f} = r\omega^2\mathbf{u}_r$.

The analytical solution of this problem is given by :

$$\mathbf{u}(r, \theta) = 0 \tag{26}$$

$$p(r, \theta) = \frac{1}{2}\omega\left(\frac{R^2}{2} - r^2\right) \tag{27}$$

We give below some results of the numerical simulation of this example. We observe that the velocity field isn't

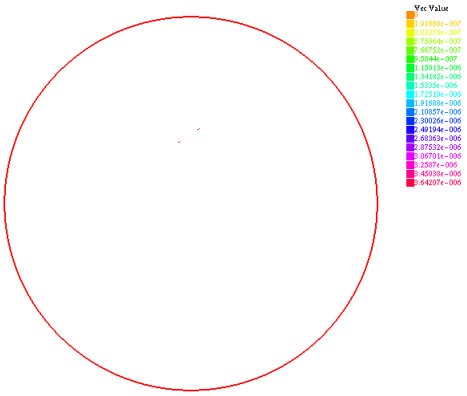

Figure 2: Velocity field in a rotating cylinder calculated using $\mathbb{P}_1 - bubble/\mathbb{P}_1$ elements

.

exactly null in this simulation (figure 2), due to numerical errors. However, the order of magnitude of its value, equal to 10^{-6}, is satisfying. We give below the L^2 errors

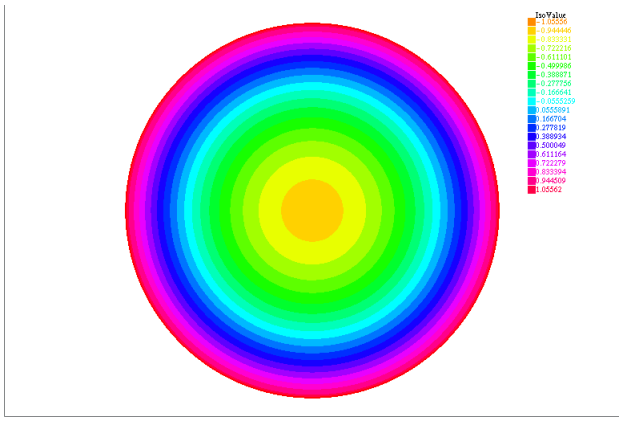

Figure 3: Pressure field in a rotating cylinder calculated using $\mathbb{P}_1 - bubble/\mathbb{P}_1$ elements

.

:

$\mathbb{P}_1 - bubble/\mathbb{P}_1$		$\mathbb{P}_2/\mathbb{P}_1$	
velocity	pressure	velocity	pressure
2.838 10^{-6}	8.709 10^{-4}	3.597 10^{-6}	8.615 10^{-4}

Table 1: L^2 errors of the rotating cylinder example

2.2.2 The Couette flow

The Couette flow is the flow of a fluid between 2 cylinders with the same axis. The inner cylinder (of radius R_1) is rotating at a velocity ω and the outer cylinder (of radius R_2) is immobile.

Here we consider that the two cylinders are sufficiently long for this problem to be 2 dimensional.
The boundary conditions are: -On the inner cylinder the velocity is fixed at $R_1.omega\mathbf{u}_\theta$. -On the outer cylinder the velocity is fixed at zero. With the subspaces P2-P1 we obtain these results for the velocity and the pressure:

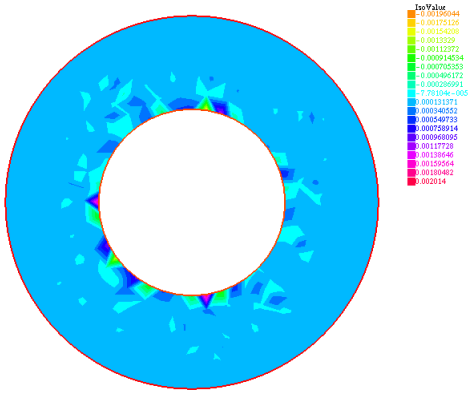

Figure 4: Pressure field of the Couette flow calculated using $\mathbb{P}_2/\mathbb{P}_1$ elements

.

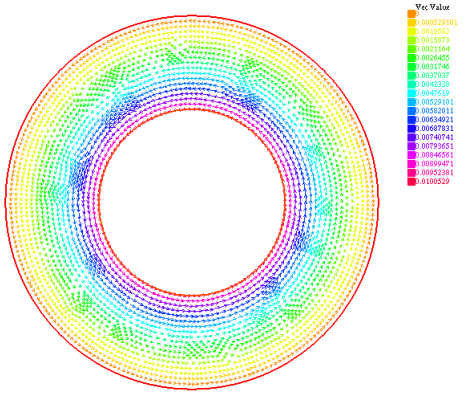

Figure 5: Velocity field of the Couette flow calculated using $\mathbb{P}_2/\mathbb{P}_1$ elements

.

We see that the velocity is consistent with the analytical solution :

$$\mathbf{u}(r,\theta) = \left(Ar + \frac{B}{r}\right)\mathbf{u}_\theta \tag{28}$$

The pressure is relatively constant, yet the analytical solution is :

$$p(r,\theta) = \frac{A^2}{8}r^2 + AB\ln(r) - \frac{B^2}{2R^2} \tag{29}$$

where $A = -\frac{\omega {R_1}^2}{{R_2}^2 - {R_1}^2}$ and $B = \frac{\omega R_1^2 R_2^2}{R_2^2 - R_1^2}$. We give in the table 2 the L^2 errors between the numerical and exact solution.

$\mathbb{P}_1 - bubble/\mathbb{P}_1$		$\mathbb{P}_2/\mathbb{P}_1$	
velocity	pressure	velocity	pressure
$3.119\ 10^{-3}$	$9.13\ 10^{-4}$	$3.118\ 10^{-3}$	$1.472\ 10^{-5}$

Table 2: L^2 errors of the Couette flow example

These simulations are obtained with a right choice of spaces for the velocity and the pressure, yet with a hasty choice like
$mathbbP_1/mathbbP_0$ the result is completely incoherent with the analytical expression In figures 6 and 7, we see the results of this simulation. The velocity field in this case has relatively high values and the vectors orientation isn't conform to physical expectation. The pressure values are not physical (order of magnitude of 10^{32}!)

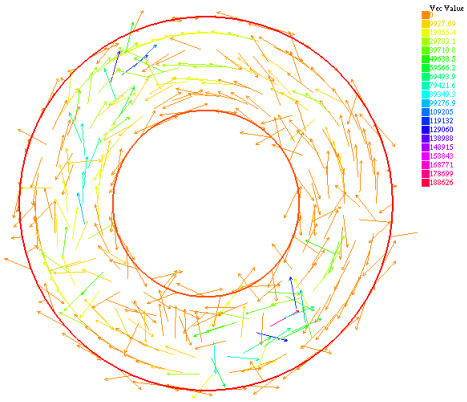

Figure 6: Velocity field of the Couette flow calculated using $\mathbb{P}_1/\mathbb{P}_0$ elements
.

2.2.3 Wind tunnel with an obstacle

In this example we consider a circular obstacle inside a wind tunnel. The box that delimits the obstacle is considered big enough to guarantee a uniform velocity equal to the entry velocity on all of it's border. The following simulation results have been calculated using the elements
$mathbbP_2/mathbbP_1$ The velocity is at its lowest value around the obstacle due to the condition of adhesion, especially in front of and behind the circle.
On the same section as the fluid we notice that the flow is very fast, this can be explained with the condition of flow conservation : equation (14)
Away from the obstacle the flow is quite uniform and verifies the border conditions.

The pressure is at its highest value just in front of the obstacle and at its lowest value just behind it. It is also

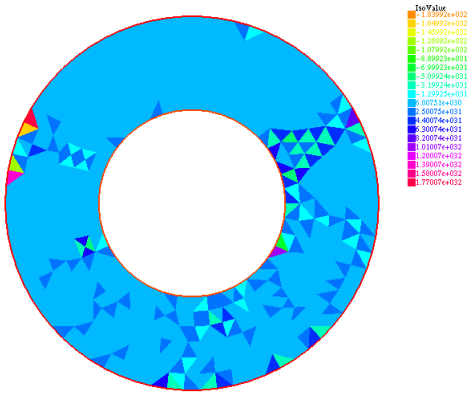

Figure 7: Pressure field of the Couette flow calculated using $\mathbb{P}_1/\mathbb{P}_0$ elements
.

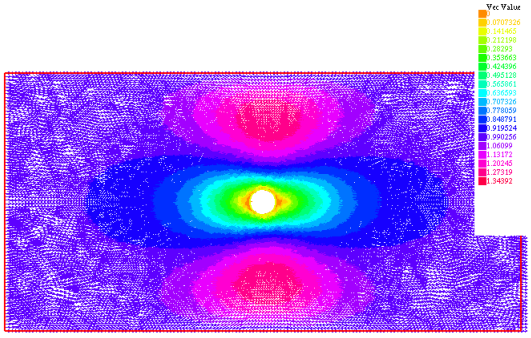

Figure 8: Velocity field of the Couette flow calculated using $\mathbb{P}_2/\mathbb{P}_1$ elements
.

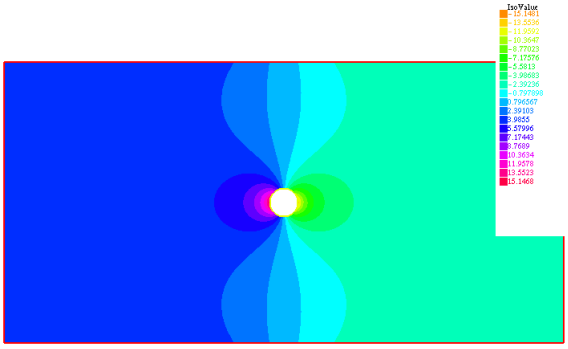

Figure 9: Pressure field of in a wind tunnel around a circular obstacle calculated using $\mathbb{P}_2/\mathbb{P}_1$ elements
.

quite uniform in the sections far from the obstacle.
We show below th pressure field calculated with $\mathbb{P}_1 - bubble/\mathbb{P}_1$. We see that the pressure contour lines in this

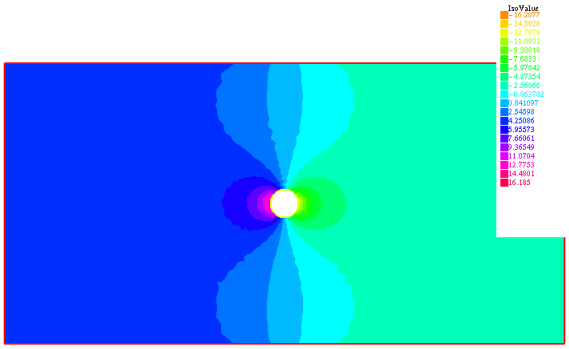

Figure 10: Pressure field of in a wind tunnel around a circular obstacle calculated using $\mathbb{P}_1 - bubble/\mathbb{P}_1$ elements
.

case show some low magnitude unphysical oscillations, due to numerical calculus errors.

2.2.4 Comparison of space choices

The most ecnonomical choice of subspaces is $\mathbb{P}_1 - bubble/\mathbb{P}_1$, because only one degree of freedom is added to the velocity on each triangle. However, it's not very precise when it comes to pressure field calculation, especially with a non-homogeneous Dirichlet Boundary condition.
$\mathbb{P}_2/\mathbb{P}_1$ provides satisfying pressure and velocity fields. However, it becomes costly in terms of calculation time when the mesh becomes too dense.
As a result, if the mesh isn't enough dense, $\mathbb{P}_2/\mathbb{P}_1$ is the wisest choice, and vice versa.

2.3 Steady non-linear Navier-Stokes simulations

After having successfully numerically simulated the Stokes flow, we simulate in this section the steady Navier-Stokes flow. It is governed by the steady version of 1, i.e :

$$Re(\mathbf{u}.\nabla)\mathbf{u} - \Delta\mathbf{u} + \nabla p = \mathbf{f} \quad \text{in } \Omega \tag{30}$$
$$\nabla.\mathbf{u} = 0 \quad \text{in } \Omega \tag{31}$$
$$\mathbf{u} = 0 \quad \text{on } \partial\Omega \tag{32}$$

We'll use two iterative methods: The Picard method and the Newton-Raphson method. Both methods' are initialized by the Stokes flow solution (i.e $Re = 0$). Then the Reynolds number is progressively increased (or the viscosity μ is decreased) until we attain the target Reynolds (or viscosity). In fact, if we directly resolve the equations with a relatively high Re, the calculations may easily diverge. The increasing step must be controlled at each iteration. Before moving to the next Re, the calculations must verify a certain convergence criterion.

2.3.1 The Picard method

The Picard method is an iterative method which consists in finding a solution to the steady Navier-Stokes equations, according to the following algorithm (seen in [14]):

$$Re(\mathbf{u}_k.\nabla)\mathbf{u}_{k+1} - \Delta\mathbf{u}_k + \nabla p_{k+1} = \mathbf{f} \quad \text{in } \Omega$$
$$\nabla.\mathbf{u}_{k+1} = 0 \quad \text{in } \Omega$$

The weak formulation of this algorithm is resolved in FreeFem++. We proceed as follows :

- We begin with a Reynolds equal to 0.
- We divide the interval separating this initial value and the target Re into equal parts that will define the steps of the increasing of the Reynolds. For exmple, if we aim to $Re = 100$, we increase it progressively by 20 at each step.
- We move to the next Reynlods if a certain convergence criterion is verified : $\| \mathbf{u}_{k+1} - \mathbf{u}_k \|_1^2 \leq \varepsilon \| \mathbf{u}_k \|_1^2$, where $\| \mathbf{u} \|_1^2 = \| \mathbf{u} \|_{\mathbb{R}^{N_h}}^2 + \| \nabla\mathbf{u} \|_{\mathbb{R}^{N_h}}^2$.We chose this norm becaue it imposes more precision on the gradient of the solution in addition to its value. The ε depends on the problem. For example, the wind tunnel with a circular obstacle requires an ordrer of magnitude of 10^{-50} for ε to function well, whereas if the obstcle is an airfoil wih a null angle of attack, this order of magnitude becomes only 10^{-10}.
- If $\| \mathbf{u}_{k+1} - \mathbf{u}_k \|_1^2 \geq \kappa \| \mathbf{u}_k \|_1^2$ (where κ is a number to choose), then we assume that the solution begins to diverge. In this case we go back to the previous Reynolds and we devide the increasing step by two.

The whole procedure is done progressively until we attain the wanted Reynolds. We give below the result of a flow around an airfoil simulation

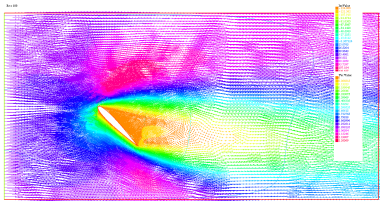

Figure 11: Velocity field and pressure contour lines of the steady Navier-Stokes flow around a NACA0012 airfoil, calculated using $\mathbb{P}_2/\mathbb{P}_1$ elements with the Picard method. $Re = 100$ and the the angle of attack is 45°
.

2.3.2 The Newton method

The Newton or Newton-Raphson method is an algorithm used to determine a zero of a function F. It is presented in [12]. It works as follows:

1. choose $u_0 \in \mathbb{R}^n$
2. for$(i = 1, i \leq n_{iter}, i++)$
   (a) solve $DF(ui)wi = F(ui)$
   (b) $u_{i+1} = u_i - w_i$

   break if $\| wi \| < \varepsilon$ where $DF(u)$ is the differential of F at the point u .

In our case we have :

$$F(\mathbf{u}, p) = \int_\Omega ((\mathbf{u}.\nabla)\mathbf{u}).\mathbf{v} + \mu\nabla\mathbf{u} : \nabla\mathbf{v} - p\nabla.\mathbf{v} - q\nabla.\mathbf{u}$$

$$DF(\mathbf{u}, p)(\delta\mathbf{u}, \delta p) = \int_\Omega ((\delta\mathbf{u}.\nabla)\mathbf{u}).\mathbf{v} + ((\mathbf{u}.\nabla)\delta\mathbf{u}).\mathbf{v} + \mu\nabla\delta\mathbf{u} : \nabla\mathbf{v} - \delta p\nabla.\mathbf{v} - q\nabla.\delta\mathbf{u}$$

The flow is characterised by the Reynolds number, we have seen that the Stokes flow is a good approximation for flows with fairly low Reynolds number.
However , in order to simulate a flow with high Reynolds number (for example Re = 200) we have to gradually augment the Reynolds number in order to obtain a physically acceptable velocity and pressure fields. Thus in order to calculate such flow we should have two loops:

- an external loop in which the Reynolds number is increased at each step (for example by decreasing the viscosity μ)
- an internal loop where the flow is calculated using the Newton method

Below is the result of a simulation of a flow around a plate using the Newton-Raphson method.

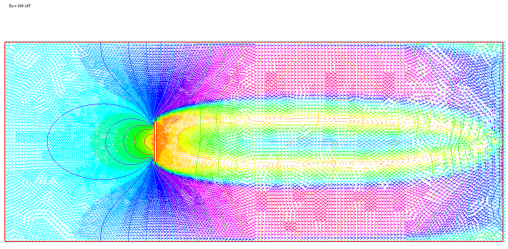

Figure 12: Velocity field and pressure contour lines of the steady Navier-Stokes flow around a vertical plate, calculated using $\mathbb{P}_2/\mathbb{P}_1$ elements with the Newton-Raphson method. $Re = 198.167$

.

2.4 Conclusion

In this work we have seen the weak formulation of a fluid motion problem which is the stokes flow.
In order to numerically calculate The pressure and velocity of such flow we had to use different subspaces for the velocity and the pressure. This justifies the appellation of mixed finite elements method.We have seen first hand how incompatible subspces provide completely wrong results.
We have also seen how to take into account the non linear term of Navier Stokes equation with two different methods: The Picard method and the Newton method.
It is important to understand the limits of this work when it comes to simulating flows with high Reynolds number.

References

[1] J.-F. Scheid : *Analyse numérique des équations de Navier-Stokes*, Cours de Master 2 Mathématiques (Recherche), Université de Lorraine (2005-2006)

[2] E. Bécache, P. Ciarlet, C. Hazard and E. Lunéville : *La méthode des élément finis, De la théorie à la pratique, II. Compléments*, Les presses de l'ENSTA (2010)

[3] M. Salaün *Equations de Navier-Stokes incompressibles*, Lecture notes, ISAE-SUPAERO

[4] S. Childress : *An Introduction to Theoretical Fluid Dynamics*, Course notes, Applied Mathematics Laboratory, Department of Mathematics, Courant Institute of Mathematical Sciences, New York University (2008)

[5] M. Fermigier : *Écoulements à petits nombres de Reynolds*, Lecture notes mécanique des fluides, ESPCI (2008-2009)

[6] L. Chen : *Inf-Sup Conditions*, Lecture notes, University of California (2014)

[7] L. Chen : *Finite Element Methods for Stokes Equations*, Lecture notes, University of California.

[8] S. Zhang : *The divergence-free finite elements for the stationary Stokes equations*, Lecture notes, Department of Mathematical Sciences, University of Delaware, USA

[9] E. Süli : *A Brief Excursion Into The Mathematical Theory Of Mixed Finite Elements Method*, Lecture notes, Mathematical Institute, University of Oxford

[10] L. P. Franca, T.J.R. Hughes and R. Stenberg : *Stabilized Finite Element Methods for the Stokes Problem*, Incompressible Computational Fluid Dynamics, Cambridge University press (1993)

[11] http://www.freefem.org/ff++/

[12] F. Hecht: *FreeFem++, Third Edition, version 3.35*, tutorial, Jacques-Louis Lions Laboratory, Pierre et Marie Curie University, Paris

[13] J. Rochat: *Résolution numérique du problème de Stokes en 3D avec l'élément fini* $\mathbb{P}_2/\mathbb{P}_1$, Study project, EPFL.

[14] C.E. SERUR: *Fast iterative methods for solving the incompressible Navier-Stokes equations*, Master of science in applied mathematics thesis, Delft Institute of Applied Mathematics (February 2013).